

Experimental investigation of intravascular OCT for imaging of intracranial aneurysms

Thomas Hoffmann¹ · Sylvia Glaßer² · Axel Boese³ · Knut Brandstädter⁴ · Thomas Kalinski⁵ · Oliver Beuing¹ · Martin Skalej¹

Received: 13 January 2015 / Accepted: 22 July 2015 / Published online: 5 August 2015
© CARS 2015

Abstract

Purpose Rupture risk assessment of an intracranial aneurysm (IA) is an important factor for indication of therapy. Until today, there is no suitable objective prediction method. Conventional imaging modalities cannot assess the IA's vessel wall. We investigated the ability of intravascular optical coherence tomography (OCT) as a new tool for the characterization and evaluation of IAs.

Materials and methods An experimental setup for acquisition of geometrical aneurysm parameters was developed. Object of basic investigation was a silicone phantom with six IAs from patient data. For structural information, three circle of Willis were dissected and imaged postmortem. All image data were postprocessed by medical imaging software. **Results** Geometrical image data of a phantom with six different IAs were acquired. The geometrical image data showed a signal loss, e.g., in aneurysms with a high bottleneck ratio. Imaging data of vessel specimens were evaluated with respect to structural information that is valuable for the characterization of IAs. Those included thin structures (intimal flaps), changes of the vessel wall morphology (inti-

mal thickening, layers), adjacent vessels, small vessel outlets, arterial branches and histological information.

Conclusion Intravascular OCT provides new possibilities for diagnosis and rupture assessment of IAs. However, currently used imaging system parameters have to be adapted and new catheter techniques have to be developed for a complete assessment of the morphology of IAs.

Keywords Intracranial aneurysm wall · Optical coherence tomography (OCT) · Rupture risk · Intracranial arterial wall

Introduction

An intracranial aneurysm (IA) is a saccular or fusiform dilation of intracranial arteries, mainly of those forming the circle of Willis and bifurcations of nearby cerebral arteries. In 6–10/100,000 inhabitants per year, an IA ruptures, which leads in the majority of cases to a subarachnoid hemorrhage (SAH) [1]. Approximately half of the patients die during the first 30 days after SAH and up to 50% of the surviving patients suffer from permanent neurological and psychological deficits [2].

In contrast to the low incidence of aneurysm rupture, the prevalence of IAs is high with 3–6% in most Western countries [3]. Due to the widespread use of magnetic resonance imaging (MRI) and computed tomography (CT) as diagnostic tools, many IAs are incidentally detected during examinations conducted for other reasons [4]. Thus, the physician is frequently facing the decision, whether the treatment—with the risk of severe complications—of such an unruptured IA is necessary to prevent SAH and its consequences, or whether observation suffices. The rupture rates of asymptomatic IAs are reportedly equaled or exceeded by

✉ Thomas Hoffmann
t.hoffmann@ovgu.de

¹ Institute of Neuroradiology, Otto-von-Guericke University, Magdeburg, Germany

² Department of Simulation and Graphics, Otto-von-Guericke University, Magdeburg, Germany

³ Department of Medical Engineering, Otto-von-Guericke University, Magdeburg, Germany

⁴ Institute of Forensic Medicine, Otto-von-Guericke University, Magdeburg, Germany

⁵ Institute of Pathology, Otto-von-Guericke University, Magdeburg, Germany

the mortality rate associated with treatment [5]. But up to date, no criteria exist that allow a reliable estimation of the rupture risk. Decision for treatment is mainly based on morphological aspects such as size, shape and location. Other factors, especially thickness and histological characteristics of the aneurysm wall, cannot be satisfactorily assessed. On the other hand, such information might change the strategy and result in fewer, potentially dangerous, therapeutic interventions. Intravascular optical coherence tomography (OCT) provides the possibility to assess vessel wall thickness as well as morphological and structural properties. To evaluate the potential of OCT to overcome this clinical problem, we investigated patient-specific aneurysms as a silicon model and the ability to illustrate aneurysm-specific structural parameters.

Intravascular OCT

OCT is an established diagnostic method in cardiology for the assessment of atherosclerotic plaques and stent appositions. The diagnostic benefit has been documented in several trials and clinical studies [6–11].

Current systems are based on the spectral-domain imaging. A swept source semiconductor laser generates near-infrared light with a wavelength of 1300 nm (near-infrared light). The swept source technique enables imaging in real time. Caused by the wavelength, a spatial resolution of less than 15 μm can be reached with good soft tissue contrasts [12]. The technique is based on a Michelson interferometer.

Near-infrared light is highly absorbed and scattered by blood. For imaging of the arterial wall, blood has to be replaced by a translucent fluid. Current systems use a liquid flush injection without occluding the vessel.

Tissue has a low absorption and scattering of near-infrared light (“near-infrared window”) [13]. Thus, a tissue penetration depth of 1–3 mm is possible with this non-ionizing radiation.

Current intravascular OCT systems create two-dimensional cross-sectional images of the vessel wall. A pullback of the catheter shaft has to be started to generate volume datasets along the catheter axis.

Clinical workflow

The workflow of a cardiac OCT catheter intervention consists of eight different steps, as shown in Fig. 1. First, different system parameters must be set. Those include, e.g., the type of flush solution (saline or contrast agent), the pullback length and velocity and a manual or automatic pullback start of the catheter shaft. Next, all instruments (guide wire, guide catheter and imaging catheter) must be positioned. The location depends on the prior defined parameters. The imaging catheter is pushed through the lumen of the guide catheter and placed more distal to the pathology in the coronary artery.

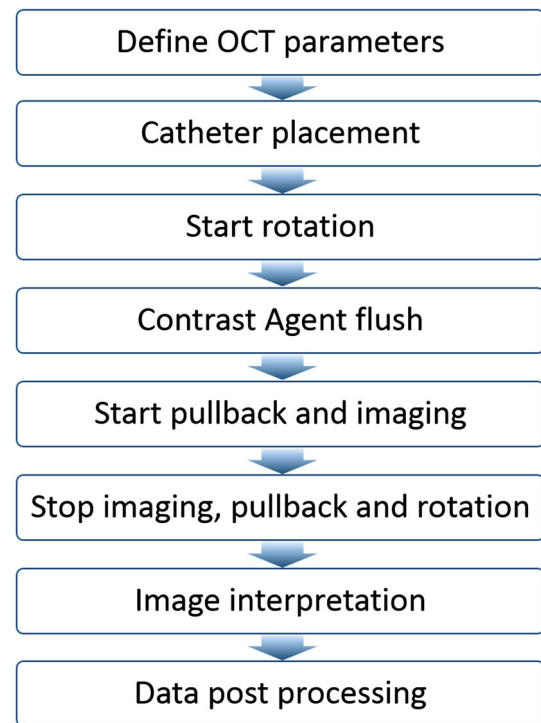


Fig. 1 Clinical workflow of an OCT catheter intervention

A guide wire with a rapid exchange system in the catheter tip can be used for an easier positioning of the OCT catheter.

In a next step, the rotation of the catheter shaft must be started and an injection of flushing solution is triggered. Using contrast agent as a flushing solution enables simultaneous C-arm angiographic imaging during the OCT pullback. The pullback and image recording start automatically, after the vessel segment is free of blood. Liquid volume and injection speed depend on the vessel under investigation.

After complete coverage of the target structure, imaging, pullback and rotation of the catheter shaft will be stopped. After postprocessing, information such as vessel diameter, thickness and composition of plaques or intima dissections can be quantified with the system.

For imaging and characterization of IA walls, the OCT parameters have to be adapted. In contrast to coronary plaque assessment or stent apposition, IAs are accompanied with different requirements and challenges for a valid characterization.

Figure 2 illustrates the adaption of OCT imaging to aneurysm walls. The thickness, borders, intramural deposits and intraluminal thrombi must be imaged. From the signal characteristics of the OCT image, information about structural differences between the normal arterial and the aneurysm wall—such as intramural hematoma, lipid content or calcified areas—should be derived.

Aneurysms show more complex geometries than healthy vessels. We describe the geometry, as illustrated in Fig. 2, by

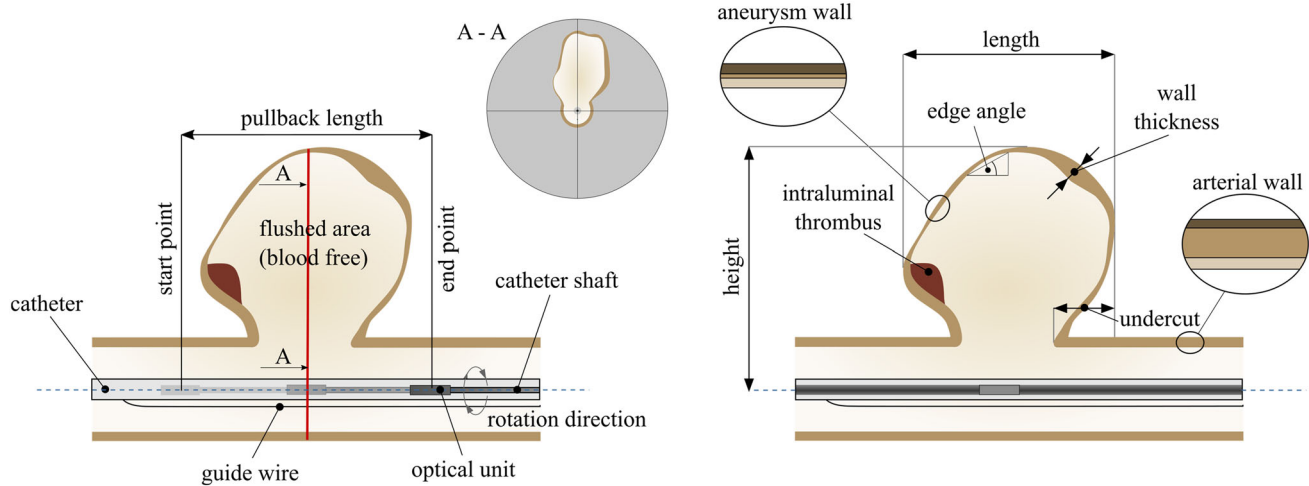


Fig. 2 Principle, requirements and parameters for catheterized OCT probing of cerebral aneurysms. *Left* schematic overview of OCT data image acquisition. The catheter shaft with probe is rotating. A pullback starts after a saline or contrast agent injection is done. The probe is pulled back from the start point (see the *light gray shape*) to the end point. The

red line shows an example of an OCT image plane. The corresponding cross-sectional OCT image is illustrated in A–A. *Right* characteristics of the aneurysm and vessel wall, which have to be considered while the imaging process

the following parameters: “aneurysm undercut” which means a vessel wall area which is located behind another vessel wall. The “edge angle” can be described as the angle between two adjacent points connected by a straight line referred to the horizontal axis. If the slope of the straight line is positive, it is named rising edge, it is called falling edge if the slope is negative. The “bottleneck value” is the ratio between maximum ostium diameter and neck diameter and is an indicator for undercuts.

The aim of our study is to examine whether intravascular OCT is suitable to provide this information.

State of the art

There is a great need for *in vivo* detection of degenerative changes of the vessel wall that arise during the development of aneurysms [14], as they may represent an important indicator of impending rupture. OCT is rated as a promising method to yield such structural information, which cannot be acquired by conventional imaging methods due to their limited spatial resolution or poor soft tissue contrast.

Nowadays, intravascular OCT is limited to applications in cardiac and peripheral vessels due to restrictions of the medical board. For neurovascular applications, only a few experimental and clinical trials were conducted in the past years.

Thorell et al. [15] created artificial coil embolized aneurysms in a canine model. OCT was used to image the aneurysm neck. The acquired images were correlated with histological findings. They concluded that OCT may be a

valuable method for follow-up studies and provides better understanding of tissue healing.

Mathews et al. [16, 17] developed an endovascular OCT catheter with a time-domain system for imaging of intracranial vessels. The study was done in animal and human vessels after explantation postmortem. A clinical trial was carried out with the healthy internal carotid artery of three patients. They showed that OCT is feasible for clinical use and can detect arterial structures. The understanding of pathologic OCT image signals allows optical biopsies of vascular tissue.

Lopes et al. [18] first imaged stent struts and arterial perforators, which could not be seen in angiography. They used a conventional OCT system and inserted the catheter by a femoral access in a human cadaver. In a second step, the brain and intracranial vessels were removed and imaged. They concluded that OCT imaging may aid in the treatment of neurovascular diseases.

Another work deals with the imaging of flow diverter struts in canine models with artificial sidewall aneurysms [19]. They conclude that OCT with its superior high spatial resolution has the ability to image malappositions.

A method to characterize mechanical properties of vessels can be done by motion estimation [20]. OCT is already able to depict dynamic processes to create elastographic investigations of plaques for the determination of their composition and mechanical properties [21].

Material and methods

In this section, the OCT system, catheter and experimental setup are described.

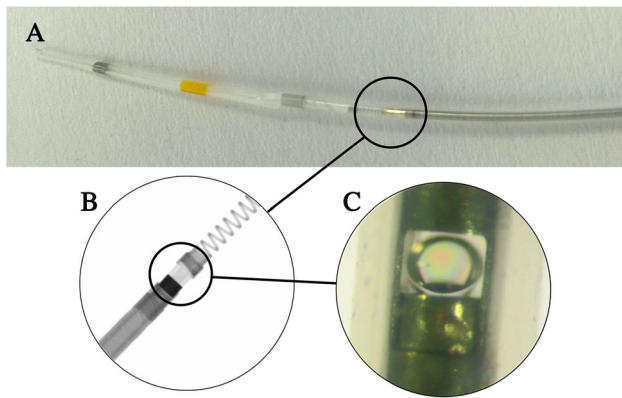


Fig. 3 TERUMO Fastview™2.6F catheter. **a** Catheter tip with rapid exchange system and optical unit (*circle*). **b** Micro-CT image of the catheter tip with lens and prism. A spring is located on top of the probe. **c** Microscopic view of the probe

OCT system

All measurements were carried out with a TERUMO LUNAWAVE™console (Terumo Corporation, Shibuya, Japan). The system is equipped with a near-infrared laser light source in the spectral domain. A maximum pullback length of 150 mm can be realized in 3.75 s. The pullback speed can be reduced stepwise from 40 to 0 mm/s. The system is real-time capable with a rate of 158 frames per second.

OCT catheter

A TERUMO Fastview™2.6F catheter was used for all measurements. It contains an optical fiber, which is rotating inside the catheter. The fiber is connected to a lens and a prism in the distal end; see Fig. 3. A linear motor in a unit, which is connected to the catheter, can pullback the fiber without changing the location of the catheter tip. A rapid exchange system at the distal end of the catheter enables the use of a guide wire.

Setup 1: Aneurysm form

We developed an individual silicone phantom to evaluate the ability to image whole aneurysms. This phantom was created using 3D angiographic datasets of patients harboring an aneurysm. From these data, sidewall and bifurcation aneurysms were segmented and analyzed. The aneurysm geometries were virtually separated from their parent vessel and added to a 175-mm-long cylinder with a diameter of 4 mm (see Fig. 4). This model was 3D printed in wax first and casted with silicone afterward.

To assess the general suitability of OCT for the imaging of IAs, we selected IAs with a wide geometrical range. The aneurysm volumes range from 8.78 mm³ for the smallest one

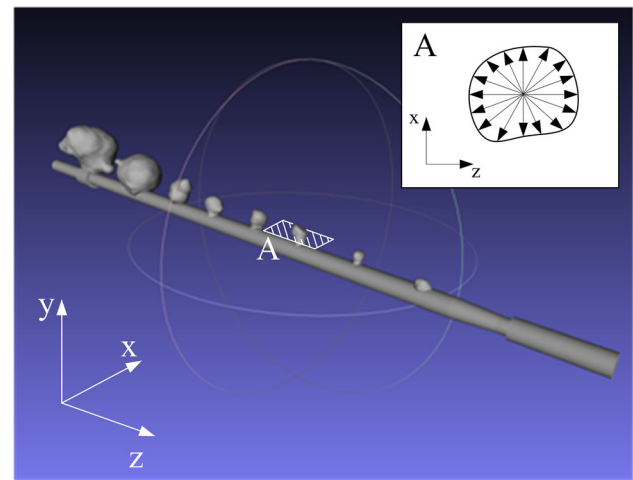


Fig. 4 Virtual cylinder with eight IAs, segmented from patient data. **a** Illustration of the measuring method for determination of dome and neck diameter. A layer with the highest diameter in x - z plane was selected. Eight circumferential measurements were carried out. In a postprocessing step, the arithmetic mean was calculated

Table 1 Extracted geometrical properties of eight selected IAs (increasing size)

Aneurysm (–)	Mean volume (mm ³)	Mean height (mm)	Aspect ratio (–)
1	8.78	2.43	0.95
2	9.24	2.66	1.34
3	26.79	4.25	1.63
4	42.99	4.07	1.33
5	54.39	5.05	1.58
6	158.77	9.02	2.09
7	946.67	11.74	1.73
8	1573.78	14.79	2.38

All measured values are mean values of 3 different measurements. Aspect ratio classification [22]: <1.6—low risk of rupture; 1.6–2.2—borderline risk; >2.2 high risk

up to 1.57 cm³ for the largest one. More parameters are displayed in Table 1. The aspect ratio (dome height/maximum neck width), which is an accepted parameter for aneurysm status, was calculated additionally. The aneurysms 3, 6 and 7 were classified as borderline risk of rupture (aspect ratio: 1.6–2.2). Aneurysm 8 was classified as high risk (aspect ratio: >2.2). Aneurysms 1, 2, 4 and 5 were assigned to a low risk of rupture [22]. All IAs were unruptured at the time of diagnostic imaging.

The experimental setup was built up in an angiography laboratory. The OCT catheter was inserted into the phantom. Afterward, model and catheter were put into a saline solution. Measurements were carried out for aneurysms 1–6, which have sufficient geometries to evaluate the imaging method. To check the pullback process of the catheter shaft, all trials were

done under fluoroscopic imaging. OCT system parameters were set to an automatic pullback of 130 mm with a velocity of 20 mm/s.

The acquired datasets were analyzed and postprocessed with the freely available software MeVisLab (MeVis Medical Solutions AG, Bremen, Germany). The postprocessing included a semiautomatic segmentation of the aneurysm contour, with a primitive thresholding and a region growing techniques. A marching cubes triangulation algorithm of the segmented 2D data stack was applied to generate a 3D mesh model of the IA. The extracted 2D and 3D image data were analyzed by experienced neuroradiologists.

For measuring the parameters neck diameter and dome diameter, a single x - z plane was selected and eight diameters were measured with MeVisLab (see Fig. 4a). The maximum, minimum and mean were extracted from those values. Height was determined by selecting a y - z plane with maximum height of the dome. Measurement was carried out from ostium to dome. Furthermore, the bottleneck (dome diameter/neck diameter) ratios of six aneurysms were calculated.

Setup 2: Structural information

In addition to the geometrical information, structural information is an indicator for the risk of rupture of an IA [14]. To check the ability of OCT to assess vascular structures, three human circle of Willis were explanted postmortem. All investigations were performed in accordance with the local ethic committee. The specimens were investigated for pathological changes of the vessel wall, e.g., plaque and aneurysms. After explantation, the preparations were flushed with saline and placed in 4 % formaldehyde. For the following OCT imaging, the preparations were fixed on a silicone plate with cannulae and embedded into a container with saline. To enter the vessel lumen with the OCT catheter, a guide wire was inserted and carefully pushed through the vessel. The OCT catheter was then advanced over the guide wire and placed in the correct position to image the selected vessel. To avoid artifacts, the guide wire was removed before imaging. For the inflation of arteries, a 5F guide catheter was placed in one of the vessels of the circle of Willis and then connected to an injector filled with saline. Flow rate was adjusted for an inflation of the current vessel of interest (4–20 ml/s). OCT system parameters were individually selected depending on the vessel length and region of interest.

Arteries with a smaller diameter than the OCT catheter were examined by positioning the catheter beside the vessel. With this technique, it was possible to image all segments of the circle of Willis (Fig. 5). The analysis of the generated datasets was carried out with MeVisLab. To validate detected abnormalities in the signal characteristics of the vessel wall, a histological investigation of the segment was done. Therefore, the preparation was embedded into paraffin and

cut into 3 μ m slices. The distances of the slices were individually selected, depending on extent of the pathology and virtual slice thickness of the OCT images. A hematoxylin and eosin (HE) stain was used. The slices were scanned with a high-resolution slide scanner (NanoZoomer, Hamamatsu Photonics, Hamamatsu, Japan).

Results

As described before, all datasets were analyzed with respect to the feasibility of probing IAs and gaining morphological information with the OCT technology.

Geometrical parameters of phantom scans

It was possible to probe and completely image aneurysms 1 and 2, as it can be seen in Fig. 6. The parameters height and diameter could be measured as well (see Table 2).

For aneurysms 3–6, it was not possible to measure the maximum height due to the limited OCT imaging diameter of 9 mm. The neck diameter could be measured for all aneurysms.

The 3D views in Fig. 6 show that the resolution in z direction, i.e., the slice distance, is not high enough to seamlessly reconstruct the aneurysm surface. Due to the pullback length and velocity, a slice thickness of 127 μ m was reached. For aneurysm number 1 and 2 were 27 and 25 slices acquired, respectively. In cases of a high gradient of the aneurysm wall along the z axis (large edge angle, see Fig. 2) and resulting high tissue thickness perpendicular to the catheter axis, it is not possible to depict the whole geometrical information.

We were able to visualize undercuts of aneurysm neck and wall in the translucent silicone phantom. An indicating parameter for undercuts is the previously described bottleneck ratio. Therefore, we measured those diameters in the image data. As shown in Table 3, the ratio varies between 1 and 1.20. For aneurysms 3–6, we measured only the maximum dome diameter which could be determined in the OCT data.

Structural information

Analysis of the ex vivo acquired datasets of intracranial vessels (Fig. 5) showed typical morphological information as described in the following. The evaluation of data was done with respect to parameters that are critical for the assessment of the rupture risk of IAs.

Intimal detachments

The ex vivo imaging of the vertebral artery showed intimal flaps in some areas. The reasons for that are unknown to us. It was probably caused by the insertion of the OCT catheter

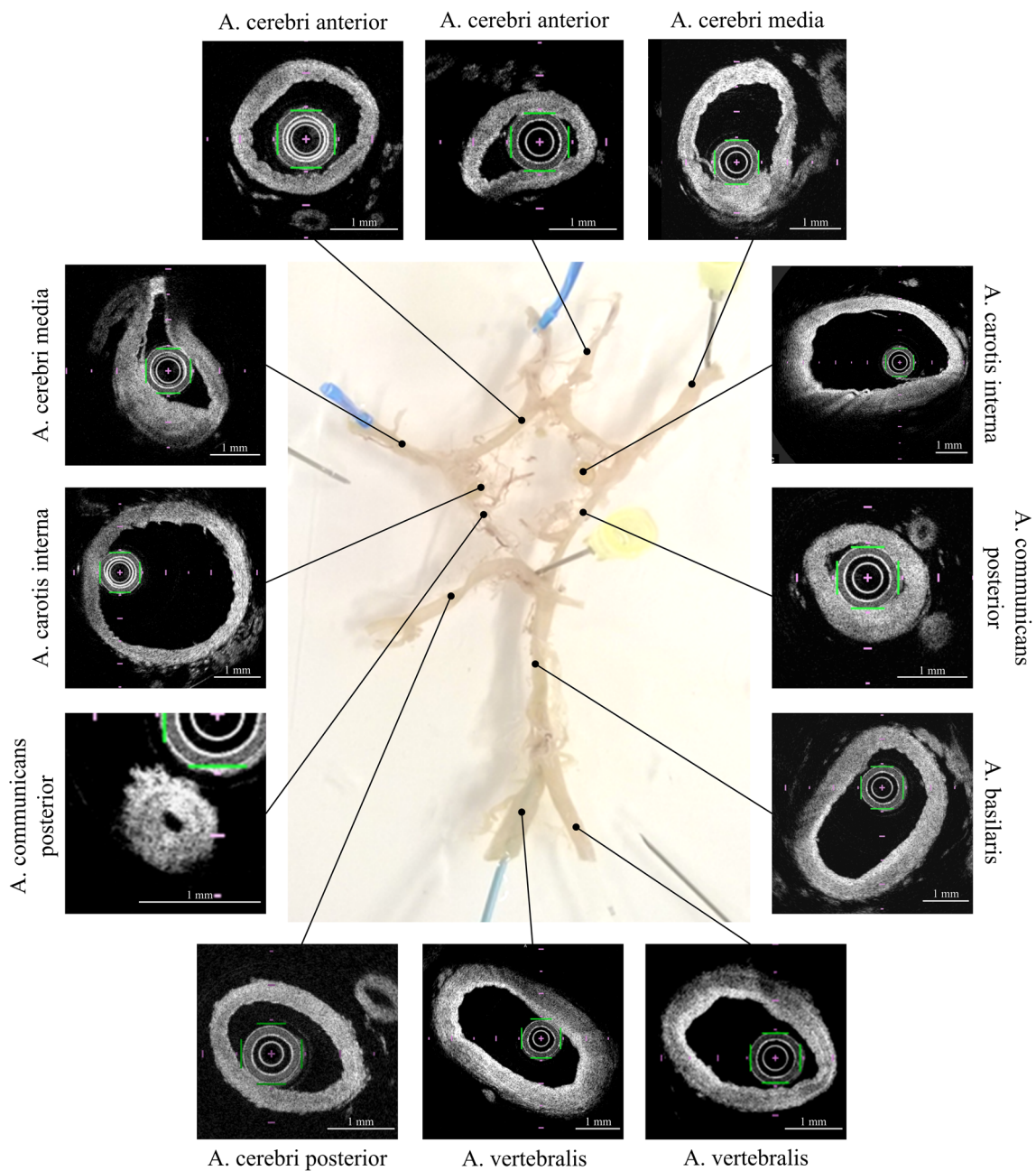


Fig. 5 Postmortem preparation of the circle of Willis. The fixated preparation is inserted in saline and attached with cannulae to a silicone plate. An OCT catheter was inserted in the vessel of interest. A

guide catheter was inserted in an adjacent vessel to flush and inflate the arteries. OCT images show the morphology of probed vessels

and the guide wire. The detached intima layer had a thickness of about $67\ \mu\text{m}$ (Fig. 7).

Intimal thickening

OCT images allow for a clear assessment of differences in intimal thickness (Fig. 8). A thickened intima was observed at branches in all imaged vessels.

Perforators

Perforating arteries could be identified ex vivo (Fig. 9). A 3D image of the artery segment shows the ability of the OCT system to image the perforator through the wall of the vertebral artery, but details of the perforator wall are lost.

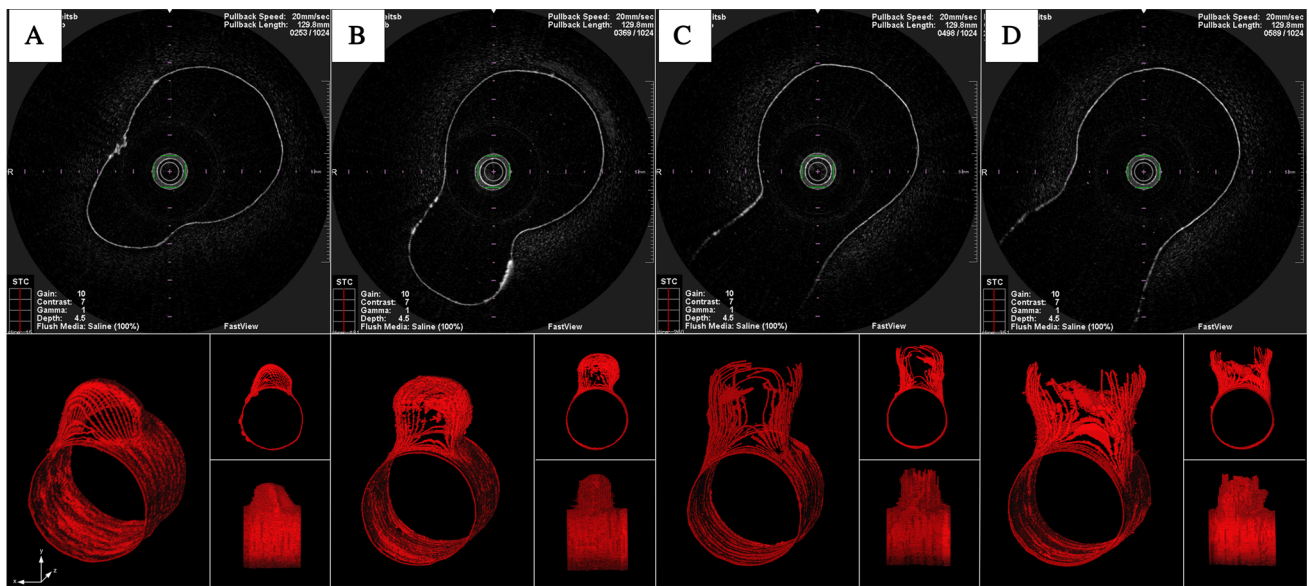


Fig. 6 OCT images (top) and 3D reconstructions (bottom) of the aneurysm silicone phantom in different views. **a, b** Acquired OCT image data of aneurysms 1 and 2 show the inner surface of the phantom. It can be seen that a loss of information is given at strongly rising and falling edges. **c, d** The maximum image diameter of the OCT system

was exceeded. The aneurysm dome could not be depicted completely. Additionally, a loss of information at areas of thick tissue (rising and falling edges) occurs. Aneurysm neck and undercuts of the dome are shown

Table 2 Geometrical parameters of six probed IAs

Aneurysm (-)	Height (mm)	Ostium diameter (mm)	Dome diameter (mm)
1	2.26	3.14	–
2	2.78	2.48	2.71
3	3.38 (max.)	2.99	3.36
4	3.58 (max.)	3.46	4.16
5	3.14 (max.)	3.93	4.40
6	3.13 (max.)	5.26	5.76

For aneurysms 3–6, the real height could not be measured caused by the maximum imaging diameter of the OCT system

Table 3 Maximum bottleneck ratios (BN) of aneurysms 1–6

BN (-)	Aneurysm					
	1	2	3	4	5	6
	1	1.09	1.12	1.20	1.12	1.10

For aneurysm 1, the ratio is calculated to a value of 1, because maximum dome diameter was identical to ostium diameter

Layered structures

As documented in literature, OCT imaging is able to depict all three layers of an artery wall. In our investigation, we were able to visualize the layered structures of all intracranial vessel preparations (see Figs. 5, 10).

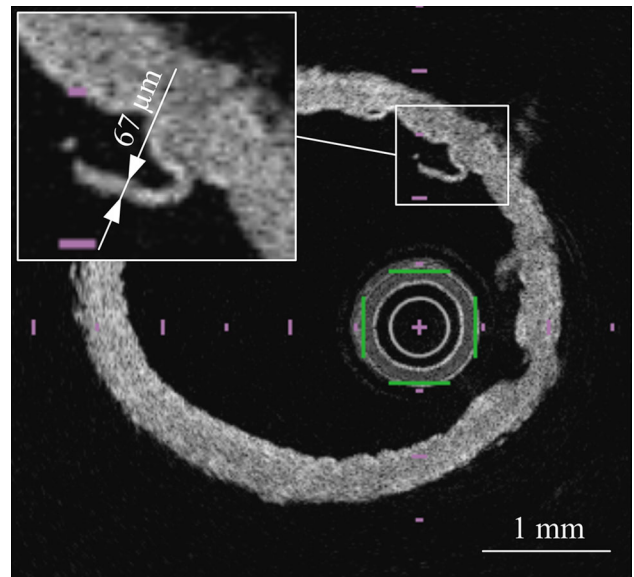


Fig. 7 OCT image of a vertebral artery shows an intimal flap with a thickness of 67 μm

Branches

The visualization of different branches with the OCT system was possible. A 3D imaging of the middle cerebral artery (MCA) shows a branch from the M1 segment to the M2 segment. As shown in Fig. 11, it is not possible to show a detailed view of the vessel wall of the adjacent vessel, caused

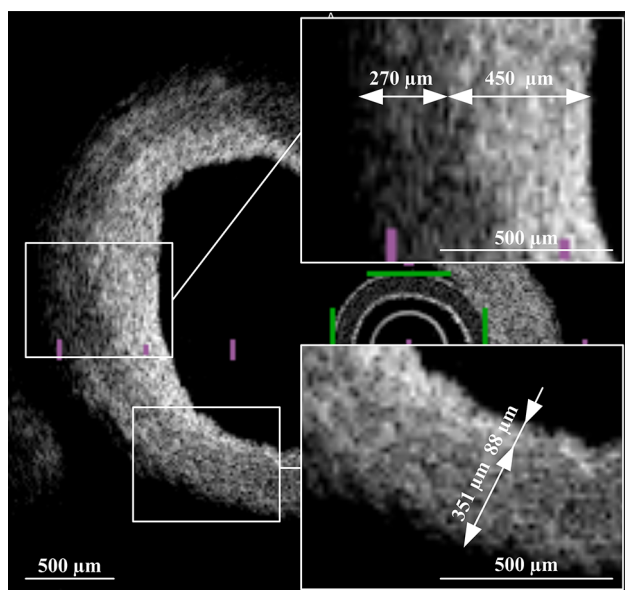


Fig. 8 Cross-sectional OCT image of a vertebral artery. A changing intima thickness from 88 μm to 450 μm can be observed

by a signal reduction through the wall of the parent vessel. It was possible to image the arterial wall in the area of the branches.

Histological information

OCT provides the possibility to differentiate normal from pathological tissue.

In our case, we investigated the generated datasets of the circle of Willis for pathological changes in the vessel wall. One internal carotid artery showed changes in the area of the intimal layer with signal loss behind. A histological investigation of the artery demonstrated a fibrous plaque with a thickness of about 500 μm (Fig. 12).

Discussion

The assessment of the rupture risk of incidentally detected IAs is of huge clinical interest, as current therapies all may lead to devastating complications. To date, the risk of future rupture of an aneurysm cannot be reliably predicted, even if several morphological parameters have been found useful by some authors. All these parameters focus on size and ratios of measured diameters, but for the estimation of the rupture risk it seems crucial to gain information about the aneurysm wall strength and intramural pathologic changes. Intravascular OCT has a very high spatial resolution and is frequently used in cardiology. Several studies proved that cardiovascular pathologies, e.g., plaques, can be well assessed by OCT, which in turn improves patient care.

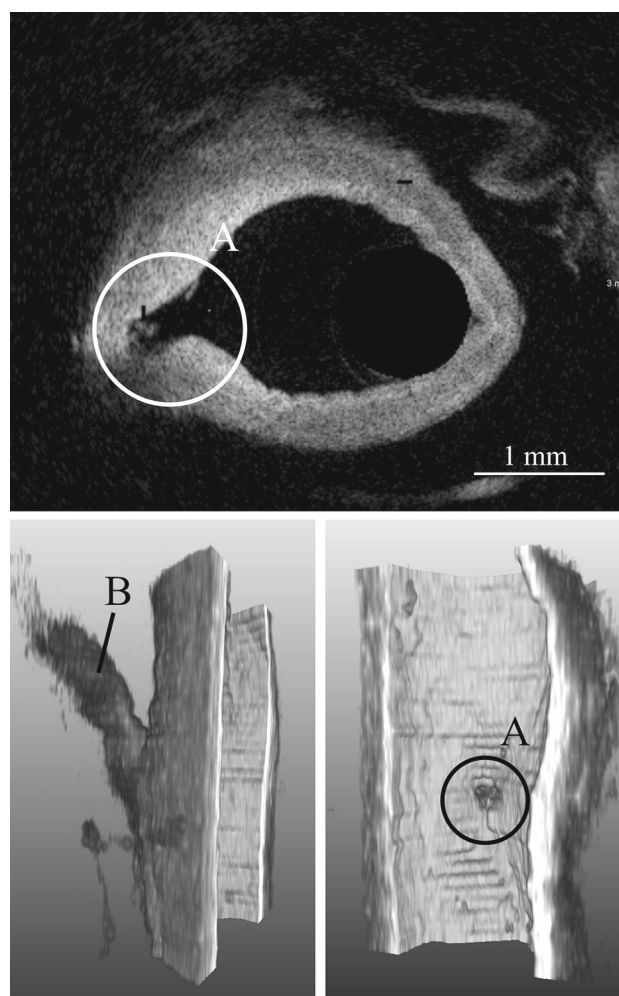


Fig. 9 Cross section and 3D illustration of a vertebral artery segment in half section. **a** Outgoing area of an arterial perforating branch. **b** Perforating vessel with lower signal and less geometrical information compared with parent vessel

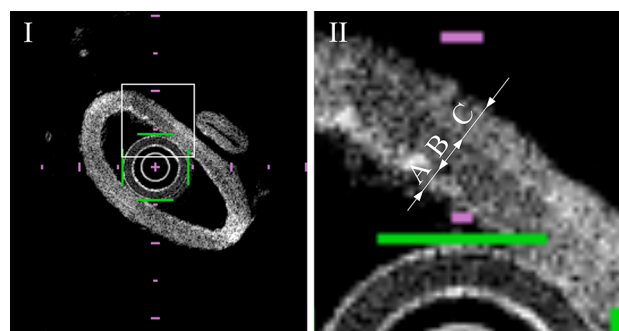


Fig. 10 Cross section of an intracranial artery. **I** Total view of the artery with discernible vessel wall layers. **II** Enlargement of a wall section from I (square) with tunica intima (A), tunica media (B) and tunica adventitia (C)

The advantage of extraordinary high spatial resolution and sufficient soft tissue contrast might be a crucial factor for an objective assessment of IAs. The imaging method pro-

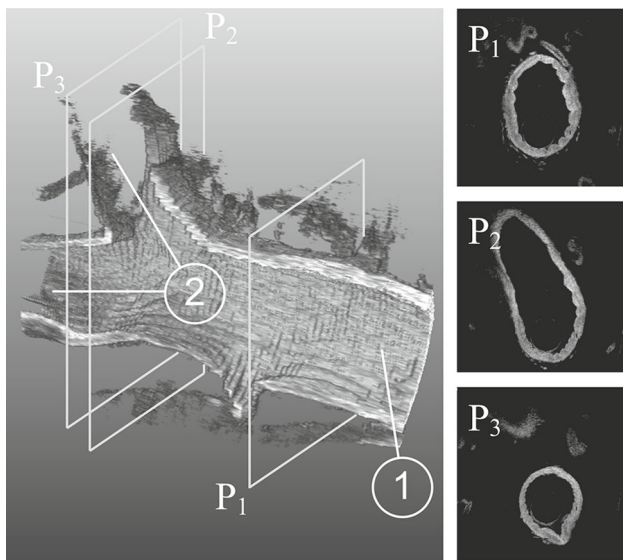


Fig. 11 Cross-sectional 2D OCT and 3D illustrations of an MCA branch. 1—Middle cerebral artery M1 segment. 2—Middle cerebral artery M2 segment. P1–P3 show cross-sectional planes of the OCT images

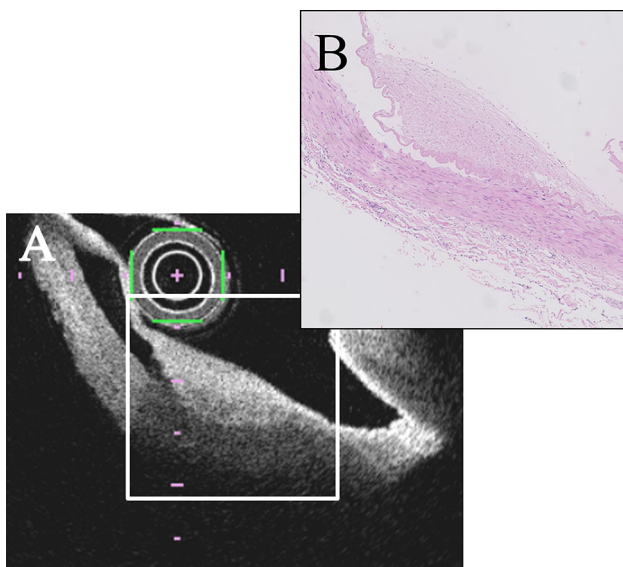


Fig. 12 OCT image of a fibrous plaque located at the internal carotid artery (ICA) communicating segment (C7). An OCT catheter is inside the vessel. Intimal detachments can be seen. Plaque structure leads to signal attenuation in the area behind. **b** Histological view of the plaque area (**a**, white square). Intimal detachments and fibrous plaque structure are observable

vides information about the vessel wall and can be used to distinguish different vessel structures. But imaging of IAs is challenging, mainly due to their complex geometry and the difficult access. Our study investigated the abilities of a current OCT system for detailed intravascular examinations of aneurysms. Focus areas were the acquisition of the correct geometry and its structural composition. Another issue,

which was not considered in our study, is the absence of blood in the aneurysms while probing. The flushing of the aneurysm might be more complex and dangerous than flushing a vessel segment for the probing of plaques. In contrast to a selected vessel segment with one major direction of blood flow, an aneurysm has a pathologic topology with irregular and complex blood flow conditions. Furthermore, aneurysms can be localized at a side wall or at a bifurcation. This fact influences the contrast flush with respect to volume and duration. Those aspects have to be further investigated.

Imaging of geometry and structure

The aim of our study was to prove the ability of probing IAs with current OCT systems, primarily used in cardiology. Therefore, the results of this study must be understood within this context.

We were able to completely image the geometry of two IAs with different shapes and sizes in a silicone phantom. The ability to capture the whole aneurysm geometry depends mainly on the catheter position in the parent vessel, the aneurysm diameter and the diameter of the ostium. The investigated silicone IAs with a maximum height of less than 4 mm showed a bottleneck ratio of maximum 1.20. Hence, it was possible to image aneurysm geometry with small undercuts from the parent vessel. Aneurysms with larger undercuts will suffer from a signal loss at the aneurysm wall caused by the absorption and scattering of the parent vessel wall. Moreover, a steep rise of the aneurysm wall (large edge angle) leads to a thicker tissue. This means that the absorption of the tissue raises and that a signal loss occurs. Thus, a correct imaging of the aneurysm geometry is impossible.

Our investigations of the ability of OCT to image arterial wall structures can be applied to IAs. We were able to image and distinguish the vessel wall layers tunica intima, tunica media, and tunica adventitia. In those layers occur the pathological changes, which lead to the formation of IAs. Thus, it is essential to assess the changes of the aneurysm wall layers to predict the rupture status of an IA. We could show that OCT enables a depiction of wall changes, i.e., an intimal thickening, an apposition of collagen and intimal flaps.

Furthermore, it is possible to visualize thin wall structures with OCT. We were able to image an intimal detachment of 67 μm . The extraordinary high spatial resolution of an OCT system enables even an imaging of thinner structures.

The imaging of vessel branches provides some indication of the ability to probe larger aneurysms with undercuts. It was shown that in areas of undercuts a signal absorption of the parent vessel strongly attenuates a signal from the adjacent vessel. Thus, information of the aneurysm vessel wall will not be visible in such cases.

Comparison with conventional imaging techniques

None of the currently established imaging modalities (e.g., CT, MRI) provide sufficient detail of aneurysm walls because of their low spatial resolution or soft tissue contrast.

Three-dimensional angiography of intracranial vessels shows only the blood flow and the inner contour of the aneurysm without information about wall thickness and structure.

MRI has the ability to show good soft tissue contrasts. Indeed, the imaging process is slower than CT and OCT depending on spatial resolution, sequence and more parameters. Current approaches with ultrahigh field MRI systems increase spatial resolution, but are not widely used in clinical routine [23].

As a result of the limited spatial resolution of current CT and MRI systems, it is not possible to generate detailed images of IAs. Signal information blur in partial volume effect with structures directly beside the aneurysm.

OCT generates more detailed images than CT and MRI but is limited in penetration depth. OCT and MRI are using non-ionizing radiation compared with CT. However, OCT catheterization is an invasive procedure which can harm the patient. Therefore, its diagnostic benefit has to be proven.

Clinical scope

The depiction of the cerebral vessel wall and its different layers offers new horizons in diagnosis and therapy of IAs. For the first time, structural information of the pathologic vessel and aneurysm wall could be potentially used for an objective diagnosis of the patient. OCT contains the possibility for a better understanding of the formation and growth of IAs. There might be new information for the decision of therapy or decision against endovascular therapy. Prior to a patient study, safety aspects of catheterization of neurovascular structures have to be examined.

Technical scope

The use of OCT as a modality for imaging aneurysms contains new focus areas in data processing, visualization and simulation. Combining angiographic data and OCT data will improve the correct imaging of the vessel morphology. This might be a basis for the extension of computational fluid dynamics (CFD) with methods of structure mechanics. A more realistic simulation of individual flow conditions and mechanical load of the aneurysm wall can help to find an objective computer-based rupture criteria.

Technical adjustments

For the implementation of those new opportunities in computer-assisted radiology and intervention, first the existing OCT systems have to be adapted to the new requirements of those pathologies. This comprises the technical revisions of the OCT catheters. Current systems are only suitable for side wall aneurysms. This is due to the fact that the laser perpendicularly probes to the catheter axis during pullback. In most cases, an IA is located at a bifurcation of a vessel. The successful application of an OCT catheter would require a pullback through the adjacent distal and the proximal parent vessel. There might be a strong signal loss while passing the wall of the parent vessel and tissue structures which are located between the parent vessel and the outer aneurysm wall. Thus, it is necessary to adapt and optimize OCT catheters for aneurysm imaging. Main focus is the design of the catheter probe; for example, for bifurcation aneurysms a forward looking OCT probe would be beneficial for imaging the ostium.

System parameters such as pullback speed and pullback length have to be adjusted to create a detailed image of the aneurysm wall.

Another important fact is the amount and volume flow of contrast agent to flush an aneurysm. Today's systems work with non-occlusive techniques. The blood flow is suppressed by the contrast agent flow. For intracranial vessels, those parameters have to be carefully examined, because changes in pressure might induce stress to the aneurysm wall and cause a rupture. In the beginnings of intravascular OCT imaging, occlusive techniques were used to suppress the blood from the region of interest. This could be an opportunity to carefully suppress blood inside the aneurysm with contrast agent. To avoid reflow from connecting vessels in the area of the circle of Willis, a balloon occlusion proximal and distal to the aneurysm could be done. Indeed, high stresses can be generated in the vessel wall which may lead to a rupture. Further investigations have to be carried out.

Conclusion

We examined the suitability of OCT to image IAs from phantom and specimen data and successfully extracted geometrical and structural properties.

Current OCT systems are able to visualize the morphology of IAs. The size and shape of the aneurysms influenced the imaging process. For side wall aneurysms, whose maximum height is less than the maximum imaging diameter of the OCT system with respect to catheter diameter, current OCT systems provide additional information of the aneurysm wall. Hence, the clinician can integrate the vessel wall thickness

and morphology in the approximation of the rupture risk and future therapy decision.

For bifurcation and larger aneurysms with a high bottleneck ratio, current OCT systems have to be technically adapted. As presented in our study, intravascular OCT shows great potential for assessing the patient-specific risk of IA rupture.

Acknowledgments This work was partly funded by the Federal Ministry of Education and Research (BMBF) and Saxony-Anhalt within the Forschungscampus STIMULATE (13GW0095A; I60).

Compliance with ethical standards

Conflict of interest There is no conflict of interest in this study.

References

- Forsting M, Wanke I (2008) Intracranial vascular malformations and aneurysms. Springer, Berlin
- Keedy A (2006) An overview of intracranial aneurysms. *McGill J Med* 9(2):141
- Mueller OM, Schlamann M, Mueller D, Sandalcioglu IE, Forsting M, Sure U (2011) Intracranial aneurysms: optimized diagnostic tools call for thorough interdisciplinary treatment strategies. *Therapeutic advances in neurological disorders*, pp. 1756285611415309
- Vernooij MW, Ikram MA, Tanghe HL, Vincent Arnaud JPE, Hofman A, Krestin GP, Niessen WJ, Breteler Monique MB, van der Lugt A (2007) Incidental findings on brain MRI in the general population. *N Engl J Med* 357(18):1821–1828
- Wiebers DO (2003) Unruptured intracranial aneurysms: natural history, clinical outcome, and risks of surgical and endovascular treatment. *Lancet* 362(9378):103–110
- Tearney GJ, Jang I-K, Bouma BE (2006) Optical coherence tomography for imaging the vulnerable plaque. *J Biomed Opt* 11(2):021002-021002-10
- Prati F, Regar E, Mintz GS, Arbustini E, Di Mario C, Jang I-K, Akasaka T, Costa M, Guagliumi G, Grube E (2010) Expert review document on methodology, terminology, and clinical applications of optical coherence tomography: physical principles, methodology of image acquisition, and clinical application for assessment of coronary arteries and atherosclerosis. *Eur Heart J* 31(4):401–415
- Murata A, Wallace-Bradley D, Tellez A, Alviar C, Aboodi M, Sheehy A, Coleman L, Perkins L, Nakazawa G, Mintz G (2010) Accuracy of optical coherence tomography in the evaluation of neointimal coverage after stent implantation. *JACC Cardiovasc Imaging* 3(1):76–84
- Kang S-J, Mintz GS, Akasaka T, Park D-W, Lee J-Y, Kim W-J, Lee S-W, Kim Y-H, Lee CW, Park S-W (2011) Optical coherence tomographic analysis of in-stent neointimal coverage after drug-eluting stent implantation. *Circulation* 123(25):2954–2963
- Farooq MU, Khasnis A, Majid A, Kassab MY (2009) The role of optical coherence tomography in vascular medicine. *Vasc Med* 14(1):63–71
- Standish BA, Spears J, Marotta TR, Montanera W, Yang VX (2012) Vascular wall Imaging of vulnerable atherosclerotic carotid plaques: current state of the art and potential future of endovascular optical coherence tomography. *Am J Neuroradiol* 33(9):1642–1650
- Fujimoto JG, Pitris C, Boppart SA, Brezinski ME (2000) Optical coherence tomography: an emerging technology for biomedical imaging and optical biopsy. *Neoplasia* 2(1):9–25
- Smith AM, Mancini MC, Nie S (2009) Bioimaging: second window for in vivo imaging. *Nat Nanotechnol* 4(11):710–711
- Frösen J, Tulamo R, Paetau A, Laaksamo E, Korja M, Laakso A, Niemelä M, Hernesniemi J (2012) Saccular intracranial aneurysm: pathology and mechanisms, (eng). *Acta Neuropathol* 123(6):773–786
- Thorell WE, Chow MM, Prayson RA, Shure MA, Jeon SW, Huang D, Zeynalov E, Woo HH, Rasmussen PA, Rollins AM (2005) Optical coherence tomography: a new method to assess aneurysm healing. *J Neurosurg* 102(2):348
- Mathews MS, Su J, Heidari E, Levy EI, Linskey ME, Chen Z (2011) Neuroendovascular optical coherence tomography imaging and histological analysis. *Neurosurgery* 69(2):430
- Mathews MS, Su J, Heidari E, Linskey ME, Chen Z (eds) (2011) Neuro-endovascular optical coherence tomography imaging: clinical feasibility and applications. *SPIE BiOS. International Society for Optics and Photonics*, pp 788341-1–788341-7
- Lopes DK, Johnson AK (2011) Evaluation of cerebral artery perforators and the pipeline embolization device using optical coherence tomography. *J Neurointerv Surg* neurintsurg-2011-010102
- van der Marel K, Gounis M, King R, Wakhloo A, Puri A (2014) P-001 high-resolution optical and angiographic CT imaging of flow-diverter stents for assessment of vessel wall apposition, (eng). *J Neurointerv Surg* 6(Suppl 1):A21
- Costalat V, Sanchez M, Ambard D, Thines L, Lonjon N, Nicoud F, Brunel H, Lejeune JP, Dufour H, Bouillot P (2011) Biomechanical wall properties of human intracranial aneurysms resected following surgical clipping (IRRA's Project). *J Biomech* 44(15):2685–2691
- Sun C, Standish B, Yang VXD (2011) Optical coherence elastography: current status and future applications. *J Biomed Opt* 16(4):043001-043001-12
- Lall RR, Eddleman CS, Bendok BR, Batjer HH (2009) Unruptured intracranial aneurysms and the assessment of rupture risk based on anatomical and morphological factors: sifting through the sands of data. *Neurosurg Focus* 26(5):E2
- Kleinloog R, Korkmaz E, Zwanenburg JJ, Kuijf HJ, Visser F, Blankena R, Post JA, Ruigrok YM, Luijten PR, Regli L, Rinkel GJ, Verweij BH (2014) Visualization of the aneurysm wall: a 7.0-tesla magnetic resonance imaging study. *Neurosurgery* 75(6):614–622